Video Article

Optical Recording of Suprathreshold Neural Activity with Single-cell and Single-spike Resolution

Gayathri Nattar Ranganathan[1], Helmut J. Koester[1]

[1]Section of Neurobiology, Center for Learning and Memory, The University of Texas at Austin

Correspondence to: Helmut J. Koester at hkoester@mail.utexas.edu

URL: http://www.jove.com/video/4052
DOI: doi:10.3791/4052

Keywords: Neuroscience, Issue 67, functional calcium imaging, spatiotemporal patterns of activity, dithered random-access scanning

Date Published: 9/5/2012

Citation: Ranganathan, G.N., Koester, H.J. Optical Recording of Suprathreshold Neural Activity with Single-cell and Single-spike Resolution. *J. Vis. Exp.* (67), e4052, doi:10.3791/4052 (2012).

Abstract

Signaling of information in the vertebrate central nervous system is often carried by populations of neurons rather than individual neurons. Also propagation of suprathreshold spiking activity involves populations of neurons. Empirical studies addressing cortical function directly thus require recordings from populations of neurons with high resolution. Here we describe an optical method and a deconvolution algorithm to record neural activity from up to 100 neurons with single-cell and single-spike resolution. This method relies on detection of the transient increases in intracellular somatic calcium concentration associated with suprathreshold electrical spikes (action potentials) in cortical neurons. High temporal resolution of the optical recordings is achieved by a fast random-access scanning technique using acousto-optical deflectors (AODs)[1]. Two-photon excitation of the calcium-sensitive dye results in high spatial resolution in opaque brain tissue[2]. Reconstruction of spikes from the fluorescence calcium recordings is achieved by a maximum-likelihood method. Simultaneous electrophysiological and optical recordings indicate that our method reliably detects spikes (>97% spike detection efficiency), has a low rate of false positive spike detection (< 0.003 spikes/sec), and a high temporal precision (about 3 msec) [3]. This optical method of spike detection can be used to record neural activity *in vitro* and in anesthetized animals *in vivo*[3,4].

Video Link

The video component of this article can be found at http://www.jove.com/video/4052/

Protocol

1. Optical Setup (Figure 1)

1. For two-photon excitation an infrared pulsed laser system with femtosecond pulses is used. A high laser output power (in some cases >2W at 890 nm wavelength) is required to offset the large losses introduced by the optical components of the system.
2. A prechirper system consisting of two prisms imparts a negative group velocity dispersion (GVD) onto the laser pulses prior to the acousto-optical deflectors (AODs) to compensate for the temporal dispersion introduced by the AODs[1].
3. Two AODs with large apertures (10 mm for a 40x water immersion objective with NA 0.8) deflect the laser beam in two dimensions.
4. A reflective diffraction grating with 100 groves/mm is placed 13 cm behind the AODs to compensate the spatial dispersion introduced by AODs when using short laser pulses.
5. The laser beam is directed with two relay telescopes into the camera port of an upright microscope.
6. Irises are placed at regular intervals for alignment of the optical components.
7. A dichroic beamsplitter in front of the objective transmits the infrared excitation light to the specimen and reflects the fluorescence light from the specimen onto a detector.
8. Epi- and transfluorescence detectors (photomultipliers, PMTs) collect fluorescence signal through the objective and - if applicable - through the condenser.
9. Colored glass filters (BG-39, 3-5 mm) are placed in front of the detectors to prevent excitation light reaching the detectors.
10. The AOD deflection angles are controlled by a computer equipped with a digital-analog-converter board (156.25 kHz clock rate), which in turn drives voltage-controlled oscillators.
11. The signal from the photomultipliers is relayed through a low-pass Butterworth filter (cut-off frequency of 100 kHz) and digitized by an analog-digital-converter (156.25 kHz clock rate) before being stored in a computer for analysis.
12. Alignment and electrical noise are tested by recording the distribution of fluorescence signals with and without laser light, at low and high gain of the photomultipliers, as well as with and without indicator. The scanner is correctly setup and shielded when the width of the distribution of the fluorescence signals at high gain and with indicator is much larger than the widths of the other distributions of fluorescence signals (**Figure 2**).

2. Experimental Procedures

1. Dithered random-access scanning relies on detection of intracellular increases in calcium. A large number of neurons can be stained using bolus injection of the ester form of a calcium indicator (for example Oregon Green 488 Bapta-1 AM) into neural tissue[5].
2. Several locations from each neuron soma are recorded, each for a short time ("dithering", 4 locations, 6.4 µsec for each location = 25.6 µsec recording time for each neuron in each cycle, **Figure 3C**). To select neurons of interest a full frame consisting of 256x256 pixels is acquired (**Figure 3A**). The center of each neuron soma to be recorded is selected manually within this image. The control software automatically adds three points at 2 µm distance around this center.
3. In each cycle, fluorescence signal is recorded from each of the 40 neurons (**Figure 3B**). This process is repeated for the entire duration of one recording (5 sec recording = 3,255 cycles, 1 cycle = 1.536 msec).

3. Online Software Ttools to Maximize Spike Detection Efficiency

1. Spike detection from fluorescence somatic calcium signals relies on a high signal-to-noise (S/N) ratio of the somatic fluorescence calcium signals. A high S/N can be achieved by increasing excitation intensity. Excitation intensity, however, can only be increased to a certain limit because of photodamage. Spike detection is high within a very small window of excitation intensities only where fluorescence signals have a high S/N but only very little photodamage is observed[3]. In order to ensure that the recorded signals are within the window of high spike detection during recordings we monitor photon rate (see equation 3.2) and decline of baseline fluorescence using online analysis.
2. Approximate photon rate per neuron is calculated from a short time window (100-200 ms) of baseline noise. Number of photons (N_λ) and photon rate ($\lambda = N_\lambda / \Delta t$) is calculated from the fluorescence values by fitting the distribution (σ) of relative fluorescence changes with the following equation:

$$\sigma(\Delta F/F) = \sqrt{\frac{N_\lambda}{2\pi}} \times \exp\left(-\frac{N_\lambda (\Delta F/F)^2}{2}\right)$$

This equation represents the poisson distribution for photon shot noise with a change of variable to relative fluorescence change: $\Delta F/F = (G*N_\lambda(t)-G*N_{\lambda,0})/G*N_{\lambda,0}$ where G denotes the cumulative gain of photomultiplier and all other electronic components. Note that this equation does not correctly determine the number of detected photons for *in vivo* recordings because there are other sources of noise (movement artifacts), in addition to photon shot noise. Nevertheless this equation is useful for *in vivo* recordings to estimate the noise.

3. Baseline fluorescence is calculated from the same time window and plotted as a function of time or trials. The average decline of baseline is kept below 0.0002/sec by adjusting laser power because spike detection rapidly declines when exceeding this limit.
4. Every 10-20 min the neuron somata positions are verified by again acquiring a full frame image. If required, recording locations are adjusted. Locations can be adjusted for all neurons at once, or for individual neurons.

4. Reconstruction of Spike Timings from Fluorescence Signals (Deconvolution)

1. The fluorescence signals resulting from neural activity often summate in time because the decay of the calcium transients is long (several hundred millisec). A deconvolution method reconstructs spike and spike timings from fluorescence signals.
2. To determine the most likely spike train underlying the recorded fluorescence signal, different models are compared. Here we used a genetic algorithm to determine the model - and thus the spike train and spike timings - with the maximum likelihood.
3. In inhomogeneous populations of neurons, the spike-evoked calcium signal can vary between neurons. For unsupervised analysis of data sets we designed an algorithm that takes into account the variation of the spike-evoked calcium signal from neuron to neuron.
4. To avoid a large number of false positive detections it is useful to constrict the allowed amplitude and decay time constant of the model of the spike-evoked calcium signal. The joint distribution of the amplitude and decay time constant of single-spike evoked calcium transients are recorded in a separate set of experiments from the same type of neurons under the same experimental conditions using simultaneous electrophysiological and optical recordings.
5. To account for slow baseline changes and to reduce computational costs of deconvolving, longer recordings are divided into several shorter traces of 1-5 sec.
6. For each neuron and each recording, the deconvolution algorithm may test a large number of models (up to 1,000,000 different models or more). To speed up deconvolution, one experiment is deconvolved on up to 10 different computers in parallel.
7. After deconvolution, the spike data is analyzed and inspected. A peri-stimulus time histogram, spike probability, and firing rate (average spike per neurons) are calculated in an automated manner.

5. Representative Results

Successful spike detection hinges on a high signal-to-noise ratio of the recorded fluorescence somatic calcium signals. Simply using high excitation rates (high laser power) can result in an adverse impact of photoeffects on biological material (photodamage). In dithered random-access scanning photodamage manifests as decreases in baseline fluorescence and decreases of the spike-evoked calcium fluorescence signals. The decrease in the spike-evoked signal can quickly result in a failure to detect spikes. There is only a very small window of excitation intensity where spike detection from fluorescence signals is high. On the higher end this window is limited by photodamage, on the lower end the fluorescence signals have a low signal-to-noise ratio. For cortical neurons in acute slices we use laser power resulting in photon rates of about 400,000-1,500,000 photon/sec when recording at around 100 µm below slice surface. When using a high-affinity indicator - here Oregon Green

488 BAPTA - 1 - this signal is sufficient to detect individual spikes. **Figure 3E** shows an example of a fluorescence signal recorded at very low excitation rate, one example of a recording within the detection window, and one at very high excitation rate.

Compared to other techniques to record neural activity with single-cell and single-spike resolution, dithered random-access scanning can record from a larger number of neurons from the same, local population, and is less invasive for example compared to tetrode/multielectrode recordings. Thus dithered random-access scanning can be used to record neural activity from many neurons to measure mutual information signaled by suprathreshold activity[6] (**Figure 4A**), changes of neural activity in a population of neurons (cortical plasticity), and propagation of suprathreshold activity through populations of neurons[14] (**Figure 4B**)

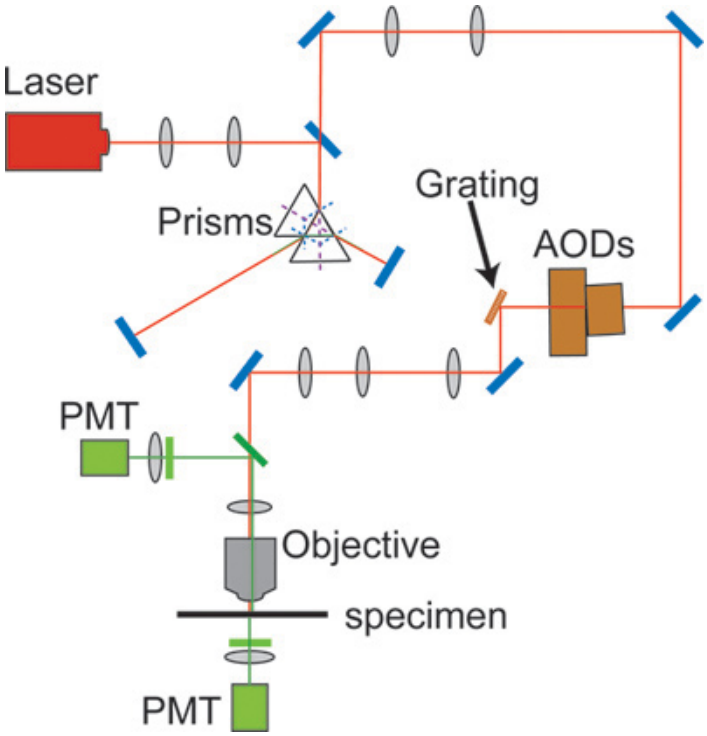

Figure 1. Optical design of the dithered-random access scanning setup.

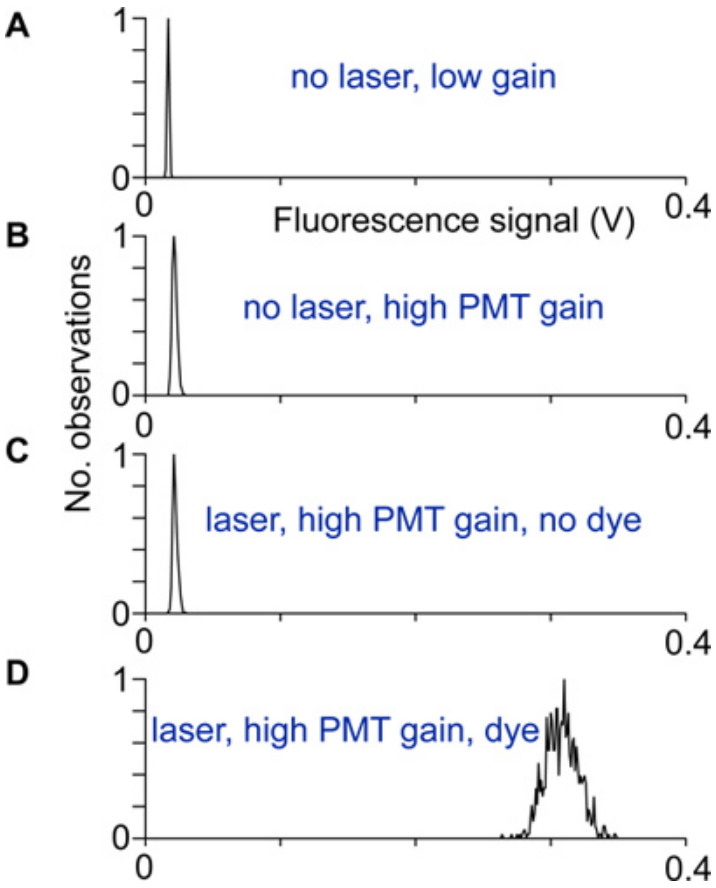

Figure 2. Alignment and testing: distributions of fluorescence signals recorded under different conditions. A) No laser light and low photomultiplier gain, B) At higher PMT gain, but no laser light, the distribution is wider because of the photomultiplier dark current. C) With the laser on and recorded at high PMT gain. A difference between the distributions in shown in B and this distribution would indicate that excitation light reaches the PMT detectors. D) The distribution of fluorescence signals recorded at high gain from neuron somata. If no other noise source contributes, this distribution arises from photon shot-noise only.

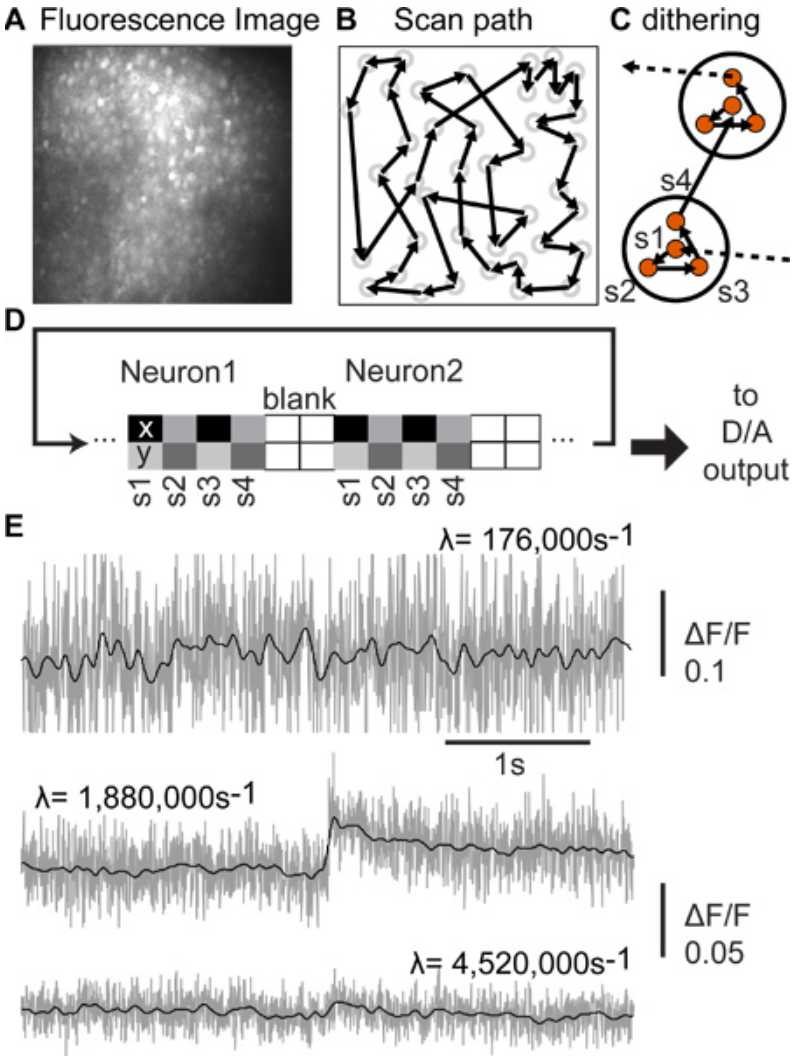

Figure 3. A) Full frame fluorescence image to detect and select neuron somata positions, B) Scan path of one cycle, C) Illustration of the dithering principle; in each soma (circle) several locations are recorded before moving the beam to the next soma, D) Illustration of the output of the two D/A channels. For each neuron soma, fluorescence signal is recorded from 4 different spots in each soma (s1-s4). The location of each spot is given by its x and y position. The x and y positions for all spots and all neurons are sent to the digital-to-analog converter in a sequential manner. While the beam is moved between two neuron somata, no signal is acquired (blank). E) Examples of fluorescence signals. Note that each example shows response to one spike (as measured with electrophysiological cell-attached recording).

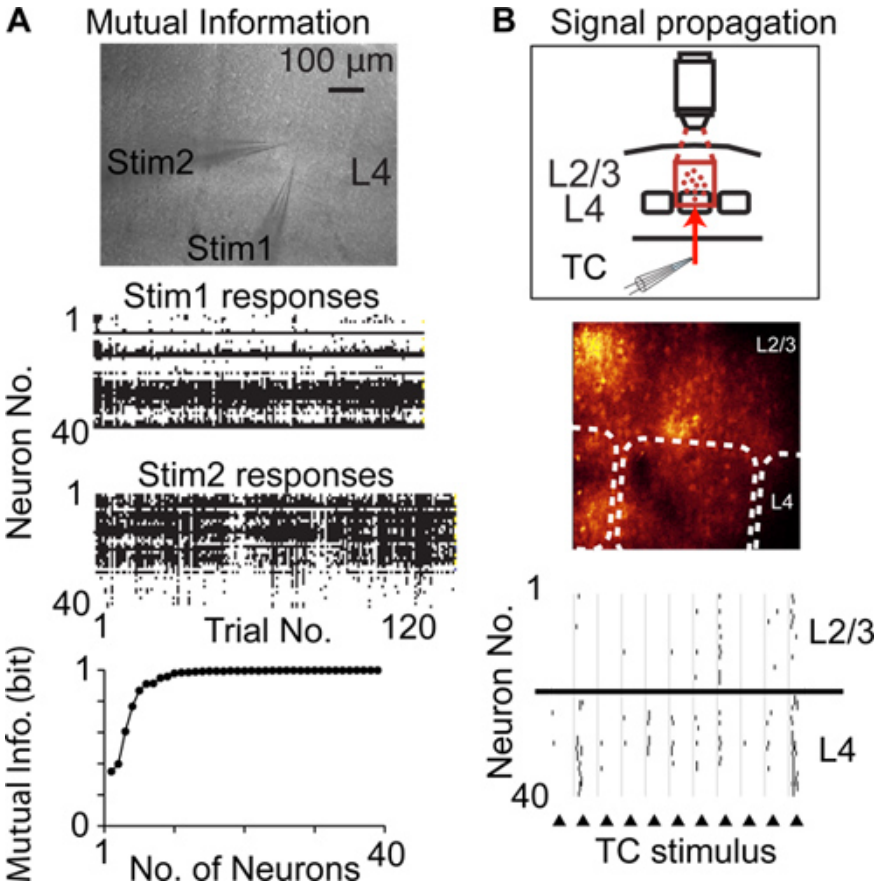

Figure 4. Studying cortical function using dithered random-access scanning. A) Measuring mutual information signaled by populations of neurons. Upper image shows photomicrograph of an acute brain slice and two stimulation pipettes placed in the same cortical column in layer 4(L4). Center graphs show neural responses for each repetition of a stimulus. Lower graph shows Shannon's mutual information signaled by the recorded population of neurons. B) Measuring propagation of suprathreshold spiking activity (signal propagation) between populations of cortical neurons. Upper graph illustrates experimental design, center image shows fluorescence image, dashed lines indicate barrel borders, lower graph shows detected spikes in response to electrical stimulation of thalamocortical fibers (triangles).

Discussion

Dithered random-access scanning indirectly detects suprathreshold spiking activity from the increases in intracellular somatic calcium associated with each spike in a neuron somata. The increases in intracellular calcium are detected by fluorescent calcium dyes. The limitations of dithered random-access scanning arise largely from of the limited signal-to-noise ratio of the calcium fluorescence signals. The signal-to-noise ratio is in turn limited by photodamage, which does not allow using high excitation rates. Because of the limited signal-to-noise ratio, spike detection fails in some neurons and can also fail for sustained and high-frequency activity. For example, when recording *in vivo*, spike detection is strongly reduced for spike rates at 40 Hz and higher [4]. The reason for reduced spike detection is that the likelihood differences for correct and incorrect models become increasingly smaller for shorter inter-spike intervals. Furthermore, dithered random-access scanning can only be used for populations of neurons where somatic increases in calcium are highly correlated with spiking activity[7] which is not the case for all brain areas and cell types (for example for granule cells in the tadpole olfactory bulb[8]).

As an alternative to the optical design we have used here a single prism can be used to compensate for spatial and temporal dispersion of the AODs instead of two prisms and a diffraction grating[4,9]. The advantage of a single prism design is a higher throughput of laser power. As an alternative to the analog control of the frequency generators we have used here, a digital control scheme can be used[1,4,10]. An analog control is simpler to implement, but it is also more prone to electrical noise distortions. Electrical noise may affect beam position and result in higher noise of the recorded calcium fluorescence signals, thus reducing spike detection efficiency. A digital control scheme, on the other hand, may be subject to digitization artifacts.

Several algorithms have been proposed for deconvolution of spikes from fluorescence signals. These include a template matching algorithm, a "peeling" algorithm[4], sequential Monte-Carlo methods[11], a maximum-likelihood method[3], and others[12]. Only few of these methods account for the differences in spike-evoked calcium signals in inhomogeneous populations. Our algorithm accounts for differences in the spike-evoked calcium signal amplitude between neurons. It thus can be used to deconvolve large data sets from inhomogeneous populations of neurons in an automated and unsupervised manner.

In vivo recordings using optical spike detection are limited to neurons in superficial layers. Furthermore, *in vivo* recordings face the additional difficulty of movement artifacts that arise from head movements in freely moving animals and heart beat in anesthetized or immobilized animals.

These movement artifacts can easily prevent spike detection because even small movements will result in fluorescence changes that exceed those evoked by spiking activity. Potential solutions include oversampling and movement corrections methods.

The last few years have seen a rapid development of the technology and the analytical methods to optically detect suprathreshold neural activity. Future technological improvements may further increase the usefulness of dithered random-access scanning by increasing the duty cycle. Both spike detection efficiency as well as the number of recorded neurons benefit from a high duty cycle. Genetically encoded calcium indicators may eliminate the bolus staining of neurons or allow staining and recording from specific subpopulations of neurons. Currently, however, the lower fluorescence changes of genetically encoded calcium indicators do not allow reliable detection of single spikes[13]. Finally, a real-time compensation for motion artifacts would allow recordings in awake and behaving animals.

Disclosures

No conflicts of interest declared.

Acknowledgements

We thank Dr. Randy Chitwood for critically reading the manuscript. This work was supported by the Whitehall Foundation and the Alfred P. Sloan Foundation grants to HJK.

References

1. Iyer, V., Hoogland, T.M., & Saggau, P. Fast functional imaging of single neurons using random-access multiphoton (RAMP) microscopy. *J. Neurophysiol.* **95**, 535-545 (2006).
2. Denk, W., Strickler, J.H., & Webb, W.W. Two-photon laser scanning fluorescence microscopy. *Science.* **248**, 73 (1990).
3. Ranganathan, G.N. & Koester, H.J. Optical recording of neuronal spiking activity from unbiased populations of neurons with high spike detection efficiency and high temporal precision. *J. Neurophysiol*. **104**, 1812-1824 (2010).
4. Grewe, B.F., Langer, D., Kasper, H., Kampa, B.M., & Helmchen, F. High-speed *in vivo* calcium imaging reveals neuronal network activity with near-millisecond precision. *Nat. Methods.* **7**, 399-405 (2010).
5. Stosiek, C., Garaschuk, O., Holthoff, K., & Konnerth, A. *In vivo* two-photon calcium imaging of neuronal networks. *Proc. Natl. Acad. Sci. U.S.A*. **100**, 7319-7324 (2003).
6. Pita-Almenar, J.D., Ranganathan, G.N., & Koester, H.J. Impact of cortical plasticity on information signaled by populations of neurons in the cerebral cortex. *J. Neurophysiol.* **106**, 1118-1124 (2011).
7. Kerr, J.N., Greenberg, D., & Helmchen, F. Imaging input and output of neocortical networks *in vivo. Proc. Natl. Acad. Sci. U.S.A*. **102**, 14063-14068 (2005).
8. Lin, B. J., Chen, T.W., & Schild, D. Cell type-specific relationships between spiking and [Ca2+]i in neurons of the Xenopus tadpole olfactory bulb. *J. Physiol*. **582**, 163-175 (2007).
9. Zeng, S., Lv, X., Zhan, C., Chen, W. R., *et al*. Simultaneous compensation for spatial and temporal dispersion of acousto-optical deflectors for two-dimensional scanning with a single prism. *Opt. Lett*. **31**, 1091-1093 (2006).
10. Otsu, Y., Bormuth, V., Wong, J., Mathieu, B., *et al*. Optical monitoring of neuronal activity at high frame rate with a digital random-access multiphoton (RAMP) microscope. *J. Neurosci. Methods*. **173**, 259-270 (2008).
11. Vogelstein, J.T., Watson, B.O., Packer, A.M., Yuste, R., *et al.* Spike inference from calcium imaging using sequential Monte Carlo methods. *Biophys. J*. **97**, 636-655 (2009).
12. Yaksi, E. & Friedrich, R.W. Reconstruction of firing rate changes across neuronal populations by temporally deconvolved Ca2+ imaging. *Nat. Methods*. **3**, 377-383 (2006).
13. Hendel, T., Mank, M., Schnell, B., Griesbeck, O., *et al.* Fluorescence changes of genetic calcium indicators and OGB-1 correlated with neural activity and calcium *in vivo* and *in vitro. J. Neurosci*. **28**, 7399-7411 (2008).
14. Ranganathan, G.N. & Koester, H.J. Correlations decrease with propagation of spiking activity in the mouse barrel cortex. *Front Neural Circuits*. **5**, 8 (2011).

